Available online at www.sciencedirect.com
SCIENCE DIRECT®
Biochimica et Biophysica Acta 1663 (2004) 97–107
BIOCHIMICA ET BIOPHYSICA ACTA
BBA
www.bba-direct.com

Investigation of the membrane localization and distribution of flavonoids by high-resolution magic angle spinning NMR spectroscopy

Holger A. Scheidt[a], André Pampel[b], Ludwig Nissler[c], Rolf Gebhardt[c], Daniel Huster[a,d,*]

[a] *Junior Research Group "Solid-state NMR Studies of the Structure of Membrane-associated Proteins", Biotechnological-Biomedical Center of the University of Leipzig, Liebigstr. 27, D-04103 Leipzig, Germany*
[b] *Institute of Experimental Physics II, Faculty of Physics and Earth Science, Linnéstr. 5, D-04103 Leipzig, Germany*
[c] *Institute of Biochemistry, University of Leipzig, Liebigstr. 16, D-04103 Leipzig, Germany*
[d] *Institute of Medical Physics and Biophysics, University of Leipzig, Liebigstr. 27, D-04103 Leipzig, Germany*

Received 14 October 2003; received in revised form 6 February 2004; accepted 17 February 2004

Available online 12 March 2004

Abstract

To investigate the structural basis for the antioxidative effects of plant flavonoids on the lipid molecules of cellular membranes, we have studied the location and distribution of five different flavonoid molecules (flavone, chrysin, luteolin, myricetin, and luteolin-7-glucoside) with varying polarity in monounsaturated model membranes. The investigated molecules differed in the number of hydroxyl groups attached to the polyphenolic benzo-γ-pyrone compounds. To investigate the relation between hydrophobicity and membrane localization/orientation, we have applied ^{1}H magic angle spinning NMR techniques measuring ring current induced chemical shift changes, nuclear Overhauser enhancement cross-relaxation rates, and lateral diffusion coefficients. All investigated flavonoids show a broad distribution along the membrane normal with a maximum in the lipid/water interface. With increasing number of hydroxyl groups, the maximum of this distribution is biased towards the lipid headgroups. These results are confirmed by pulsed field gradient NMR measurements of the lateral diffusion coefficients of phospholipids and flavonoids, respectively. From the localization of different flavonoid protons in the membrane, a model for the orientation of the molecules in a lipid bilayer can be deduced. This orientation depends on the position of the polar center of the flavonoid molecule.

Keywords: Flavone; Chrysin; Luteolin; Myricetin; Luteolin-7-glucoside; ^{1}H MAS NOESY; PFG NMR; Lipid peroxidation

1. Introduction

Flavonoids are polyphenolic benzo-γ-pyrone compounds that belong to a class of water-soluble plant pigments. More than 6000 different flavonoid molecules have been identified; they occur in vegetables, fruits, and beverages such as beer, wine, tea, and fruit drinks. These molecules have been shown to exhibit antibacterial, anti-inflammatory, antiallergic, antimutagenic, antiviral, antineoplastic, anti-thrombotic, cholesterol biosynthesis modulating and vasodilatory activity [1–5]. In animal models, flavonoids have revealed an anticancer activity [6]. As antioxidants, flavonoids are suggested for the prevention and treatment of oxidative damages of lipoprotein particles and cell membranes. Flavonoids have an ability to scavenge hydroxyl radicals, superoxide anions, and lipid peroxy radicals [7]. Epidemiological studies also support the positive effect of flavonoids on human health [7].

In order to understand the various beneficial effects of flavonoids on health mentioned above, more studies related to structural aspects of the flavonoid interaction with biological or biomimetic systems have to be carried out. The mechanism of some of the described biological effects may involve interactions of flavonoids with the cell membranes. Therefore, several studies have dealt with the influence of flavonoids on membrane structure and dynamics [8–13]. In these investigations, the propensity of flavonoids towards the lipid membrane has been demonstrated. For instance, very different partitioning of flavonoids at a water/olive oil interface has been observed in dependence of the polarity of these molecules [11]. Such measurements have been sup-

* Corresponding author. Institute of Medical Physics and Biophysics, University of Leipzig, Liebigstr. 27, D-04103 Leipzig, Germany. Tel.: +49-341-97-15706; fax: +49-341-97-15709.
E-mail address: husd@medizin.uni-leipzig.de (D. Huster).

0005-2736/$ - see front matter © 2004 Elsevier B.V. All rights reserved.
doi:10.1016/j.bbamem.2004.02.004

ported by calculations of partition coefficients of flavonoids at the octanol/water interface [14].

Phenolic hydroxyl groups provide easily donatable hydrogen atoms and, together with the stability of the remaining phenoxyl radical, flavonoid molecules are prototypic chain-breaking, free radical scavenging antioxidants [10]. Especially the 3-hydroxyl group in combination with a 2, 3 double bond has been reported to improve antioxidant efficiency [15]. This suggests flavonoids to be located in close proximity to the double bonds of the cell membrane lipids to fully exert their antioxidant potential. However, the precise location of these molecules in the membrane has been controversially discussed. Most studies assume a localization of flavonoids in the lipid/water interface of the membrane [8,9,12,13]. However, by fluorescence anisotropy measurements, Arora et al. [10] concluded that flavonoids partition preferentially into the hydrophobic core of the membrane.

The variety of substituents on the flavonoid molecules largely influence their physicochemical properties such as dipole moment or hydrophobicity, and thus determine the partitioning into lipid membranes. Therefore, we have systematically investigated the membrane partitioning of four flavonoid molecules from the flavone and flavonole subclasses with a varying number of hydroxyl groups (Fig. 1). Using modern NMR techniques, the localization and distribution of these molecules with respect to the membrane normal could be quantitatively determined. Since most of the flavonoids occur in nature not in the free but rather in the glycosylated forms, we extended our study to luteolin-7-glucoside.

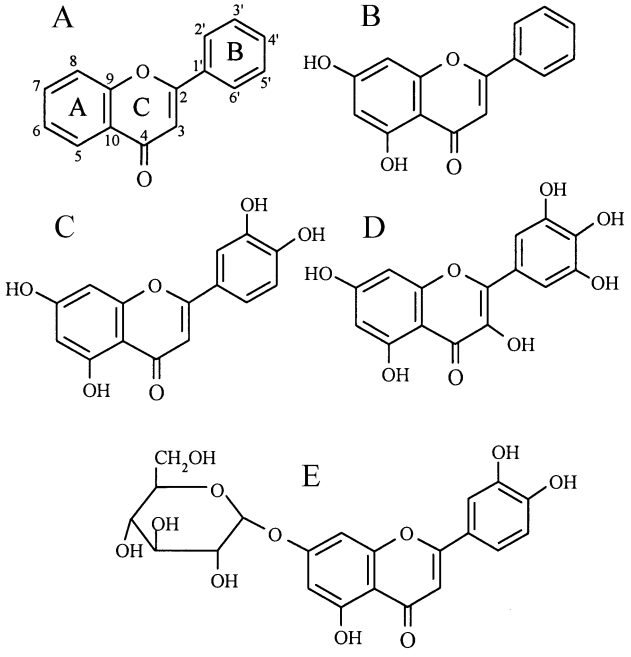

Fig. 1. Chemical structure of the four flavonoids investigated in this study (A—flavone, B—chrysin, C—luteolin, D—myricetin) and luteolin-7-glucoside (E).

Recently, new NMR tools have been developed to study the interaction of small molecules with lipid membranes [16–20]. Application of the magic angle spinning (MAS) technique allows acquiring ^{1}H NMR spectra of lipid membranes with a typical line width on the order of 20 Hz [21]. Such good spectral resolution and long spin-lattice relaxation times allow to acquire two-dimensional nuclear Overhauser enhancement spectra (NOESY) to probe spatial proton–proton contacts for structural studies similar to solution NMR applications [22]. However, NOESY spectra of lipid membranes showed crosspeaks between all lipid signals even between segments from the headgroups and the chain ends. Therefore, it was concluded that these crosspeaks are the result of spin diffusion along the lipid molecules and the merit of NOESY studies of lipid membranes was questioned [23,24].

However, recent work revisited this issue by quantitative determination of cross-relaxation rates [25]. The main result of this study was that cross-relaxation in lipid membranes is almost entirely of intermolecular origin, which qualifies this method to study the interaction of small molecules with membranes and lateral lipid organization. Since the observed cross-relaxation rates are small, the effect of spin diffusion can safely be neglected for short mixing times of a few hundred milliseconds. Further, by specific deuteration of lipid chains it was shown that spin diffusion is a very inefficient mechanism for magnetization transfer [26]. Rather, direct intermolecular contacts in highly disordered liquid crystalline membranes are responsible for the lipid–lipid cross-relaxation, which is in good agreement with modern membrane models revealed by diffraction work [27,28] and molecular dynamics simulations [29,30]. Therefore, NOESY cross-relaxation rates can be interpreted as contact probabilities between interacting protons of neighboring molecules. Thus, a number of ^{1}H MAS NOESY studies have been published studying lateral lipid organization [31] and the interaction of peptides [32–35] or small molecules [16–20,36] with lipid membranes.

In this study, we have investigated the interaction of different flavonoid molecules of varying polarity with monounsaturated zwitterionic lipid model membranes. From ^{1}H ring current-induced chemical shifts and NOESY cross-relaxation rates, the localization and orientation of these molecules in the lipid membrane could be determined. Diffusion measurements by pulsed field gradient (PFG) NMR in combination with MAS [37,38] support these results. Biological implications of the flavonoid–membrane interaction are discussed.

2. Materials and methods

2.1. Materials

1-Palmitoyl-2-oleoyl-*sn*-glycero-3-phosphocholine (POPC) was purchased from Avanti Polar Lipids, Inc.

(Alabaster, AL). Flavone, chrysin, luteolin, luteolin-7-glucoside, and myricetin were purchased from Carl Roth GmbH, Karlsruhe. All chemicals were used without further purification. The chemical structures of the four flavonoid molecules and luteolin-7-glucoside investigated in this study are shown in Fig. 1.

2.2. Sample preparation

For the MAS NMR measurements, mixtures of phospholipids and flavonoids were co-dissolved in chloroform (flavone) or a chloroform/DMSO mixture (chrysin, luteolin, luteolin-7-glucoside, myricetin) at the respective molar ratios. After evaporating the chloroform under a stream of nitrogen, the samples were redissolved in cyclohexane and lyophilized at high vacuum to obtain a fluffy powder. After hydration with 40 wt.% D_2O, the samples were equilibrated by freeze-thaw cycles and gentle centrifugation. For the ^{1}H MAS NMR experiments, the samples were transferred into 4-mm HR MAS rotors with spherical Kel-F inserts.

2.3. Solution NMR measurements

For assignment of the ^{1}H NMR signals of the flavonoid molecules, ^{1}H–^{13}C heteronuclear multiple quantum coherence (HMQC) spectra were acquired in DMSO-d_6 using a solution DRX600 NMR spectrometer (Bruker BioSpin GmbH, Rheinstetten), operating at a resonance frequency of 600.1 MHz for ^{1}H and 150.9 MHz for ^{13}C. Standard gradient HMQC spectra were acquired, using 90° pulse lengths of 8.2 and 14.5 μs for ^{1}H and ^{13}C, respectively. The ^{13}C peak assignments were taken from literature [39,40].

2.4. ^{31}P and ^{2}H NMR measurements

The static ^{31}P NMR membrane spectra were acquired on a Bruker DRX600 spectrometer operating at a resonance frequency of 242.8 MHz for ^{31}P using a Hahn-echo pulse sequence. A ^{31}P 90° pulse length of 7 μs, a Hahn-echo delay of 50 μs, a spectral width of 100 kHz, and a recycle delay of 2 s were used. Continuous-wave proton decoupling was applied during signal acquisition.

^{2}H NMR spectra were recorded on a Bruker Avanve 400 NMR spectrometer operating at a resonance frequency of 61.2 MHz for ^{2}H using a double channel solids probe equipped with a 5-mm solenoid coil. The ^{2}H spectra were accumulated at a spectrum width of 500 kHz using a phase-cycled quadrupolar echo sequence [41] and a relaxation delay of 500 ms. The two 3-μs π/2 pulses were separated by a 60-μs delay. Spectra were analyzed and order parameters were calculated as described in detail in Refs. [31,42,43]. Average order parameters were calculated by adding all order parameters and dividing them by the number of deuterated groups in the chain.

2.5. ^{1}H MAS NMR spectroscopy

^{1}H MAS NMR spectra were acquired on a Bruker DRX600 NMR spectrometer using a 4-mm HR MAS probe with pulsed field gradient capabilities at a spinning speed of either 8 kHz for NOESY NMR or 6 kHz for PFG NMR. Typical π/2 pulse lengths were 8.5 μs. A ^{2}H lock was used for field stability. All ^{1}H NMR spectra were referenced with respect to the terminal methyl group of the lipid chains at 0.885 ppm of a POPC sample in the absence of flavonoid molecules.

Two-dimensional ^{1}H MAS NOESY spectra [44] were acquired at various mixing times (between 1 and 600 ms). The dwell time of the indirect dimension was set equal to one rotor period to avoid folding of spinning side bands into the centerband region of the 2D NOESY spectra. Typically, between 512 and 1024 data points were acquired in the indirect dimension with 8 or 16 scans per increment at a relaxation delay of 3.5 s.

The volume of the respective diagonal and crosspeaks was integrated using the Bruker XWINNMR software package. NOE build-up curves were fitted to a spin pair model yielding cross relaxation rates (σ_{ij}) according to Ref. [45]:

$$A_{ij}(t_m) = (A_{jj}(0)/2)(1 - \exp(-2\sigma_{ij}t_m))\exp(-t_m/T_{ij}). \quad (1)$$

The variable $A_{ij}(t_m)$ represents the crosspeak volume at mixing time t_m and $A_{jj}(0)$ the diagonal peak volume at mixing time zero. The value $1/T_{ij}$ defines a rate of magnetization leakage towards the lattice. Cross-relaxation rates were obtained from fitting of experimental crosspeak volumes at varying mixing times to Eq. (1) using the nonlinear regression curve fitter in Origin (OriginLab Cooperation, Northampton, MA).

2.6. Diffusion measurements by PFG NMR

Diffusion measurements were performed under MAS conditions and using the stimulated echo sequence with bipolar gradient pulses and eddy current delay before detection [46]. Gradients were applied in sine-shaped manner with duration of 2.5 ms each and consecutively increasing the strength up to 80% of the maximum value (0.54 T/m). The relaxation delay between recording a signal was set to 11 s. A delay of 500 μs between gradient pulse and radio frequency pulse was used. The gradient was calibrated using a spherical water sample and measuring the water diffusion coefficient.

In a PFG NMR experiment, the observed signal amplitude is sensitive to translational motion of the spin of interest. For data analysis, the spin echo intensity was plotted as a function of observation time and fitted using a

two-dimensional diffusion model as described in Ref. [37]. The spin-echo attenuation $\Psi(k)$ is expressed by

$$\Psi(k) = \frac{1}{2}\int_0^{\pi} \exp\{-k^2 D_L \sin\Theta\}\sin\Theta \mathrm{d}\Theta \quad (2)$$

where D_L is the lateral diffusion coefficient and k is a function of gyromagnetic ratio, gradient duration, gradient strength, and observation time. To fit the observed spin-echo attenuation the integral in Eq. (2) was approximated by a sum of 256 terms equally spaced between $0 \le \Theta \le \pi$ and the lateral diffusion coefficient was obtained as a fit parameter.

3. Results

3.1. Flavonoid-membrane interaction by ^1H MAS NMR

^{1}H MAS NMR spectra of POPC membranes in the presence of different flavonoids are shown in Fig. 2. Both lipid and flavonoid signals are well resolved. The assignments of the flavonoid ^{1}H signals were determined from ^{1}H–^{13}C HMQC spectra of DMSO-d_6 solutions of the respective flavonoid while the ^{13}C chemical shifts are known from literature [39,40]. Depending on the number of hydroxyl groups, characteristic chemical shifts are observed for the different flavonoid molecules.

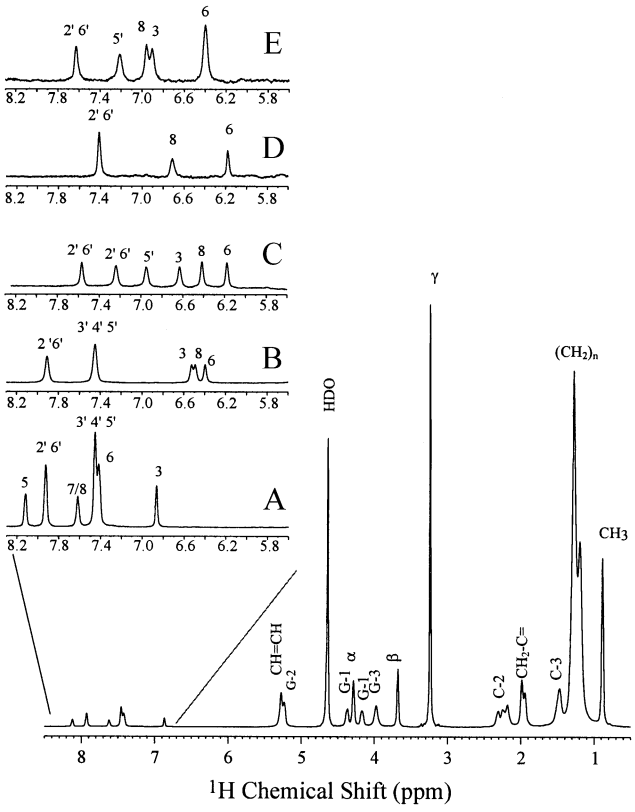

Fig. 2. ^{1}H NMR spectra (600 MHz) of POPC multilamellar membranes with 25 mol% flavone. At a water content of 40 wt.%, a temperature of 30 °C, and a MAS spinning frequency of 8 kHz. The assignment of the lipid peaks is given according to Ref. [36]. The inset shows the downfield region of the POPC spectra in the presence of 25 mol% flavone (A), chrysin (B), luteolin (C), myricetin (D), and luteolin-7-glucoside (E).

In the presence of the flavonoids, the POPC lipid signals are slightly shifted to higher magnetic fields. These shifts are due to the ring current effect of the delocalized π-electron system of the flavonoid ring structures. The magnitude of the chemical shift changes of the lipids signals depends on the proximity of the lipid protons to the aromatic ring system, while the sign of these changes depends on the orientation of the aromatic ring with respect to a lipid proton. Therefore, the aromatic ring current-induced chemical shift changes of the lipid segments provide a measure for the average location of the flavonoids. Large induced chemical shifts indicate strong lipid/flavonoid interactions. Plotted against the molecular axis of a phospholipid molecule, these induced chemical shift values provide a measure for the transverse distribution of a flavonoid in the membrane as shown in Fig. 3.

According to this data, all lipid segments are influenced by the presence of flavonoids indicated by a ring current induced chemical shift. This can be interpreted that all flavonoid molecules show a broad transverse distribution in the lipid membrane. The magnitude of the induced chemical shift values provides information about the probability of a specific location. All flavonoids are localized in the lipid/water interface of the membrane defined by the upper chain/glycerol/headgroup region. However, the distribution is biased towards the membrane center for flavone (A) and chrysin (B) and towards the aqueous phase for luteolin (C) and myricetin (D), respectively. The largest ring current-induced shifts are observed for flavone, indicating strongest interactions with lipid molecules. This suggests a distibution of the flavonoids in the membrane according to the polarity of the respective flavonoid. The most apolar flavone is located deeper in the membrane while increasing polarity due to an increasing number of hydroxyl groups provides the flavonoids a higher propensity towards the aqueous phase. In the presence of flavone, the signal of the chain methylenes ($(CH_2)_n$) is split and two different induced chemical shift values are observed. The different magnitudes in the induced chemical shift values might indicate packing differences in the flavonoid/POPC membranes.

The ring current induced shifts can be either upfield or downfield depending on the average orientation of the aromatic ring plane with respect to a lipid proton [47]. The upfield shift induced by the ring current of the aromatic flavonoids observed in our measurements indicates that the lipid protons are located above the ring plane. This suggests a parallel orientation of the long axis of the flavonoid molecules with the lipid director and, most likely, axially symmetric reorientations of the flavonoids about their long axis.

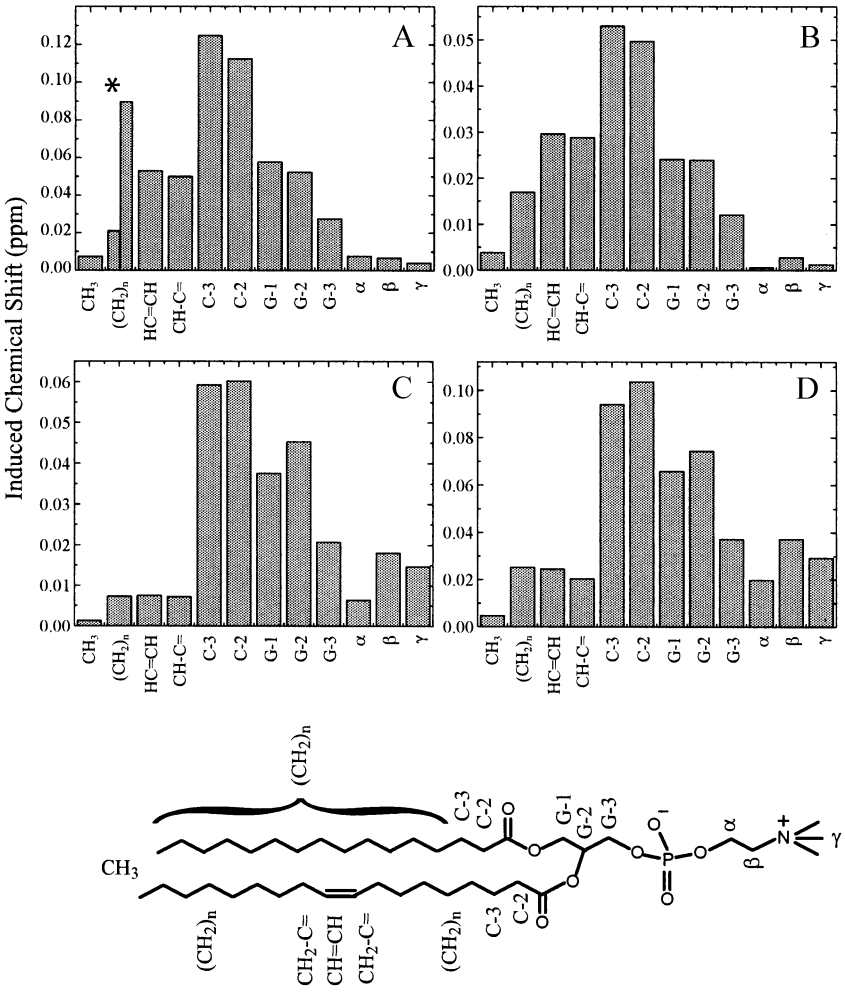

Fig. 3. Aromatic ring current induced chemical shift changes of the POPC lipid signals in the presence of flavonoids (A—flavone, B—chrysin, C—luteolin, D—myricetin). In the presence of 25 mol% flavonoid, the POPC signals are shifted downfield. The maximum induced chemical shift value indicates the most likely location of the aromatic ring system of the flavonoid with respect to the membrane normal. In the presence of flavone (A), a splitting of the lipid methylene peak $(CH_2)_n$) of POPC has been observed. The induced chemical shift values for both peaks are given (highlighted by an asterisk).

^{1}H MAS NOESY spectra provide further insight into the location and orientation of flavonoids in zwitterionic membranes. Fig. 4 shows the aromatic region of a NOESY spectrum of POPC/luteolin at a mixing time of 300 ms. All luteolin signals show intense crosspeaks with all lipid resonances. The crosspeak intensity provides a measure of the interaction strength between lipid and flavonoid protons, however, since different numbers of protons contribute to each magnetization transfer, only a quantitative analysis of cross-relaxation rates provides quantitative information about lipid–flavonoid contacts [25].

In Fig. 5, the cross relaxation rates of the 2′ /6′ protons (ring B, see Fig. 1) of the flavonoids with POPC lipid segments are plotted. Highest cross-relaxation rates indicate high contact probabilities between the interacting protons. Plotted along the molecular axis of a POPC molecule, the distribution profile of the B ring of the flavonoids in the membrane can be obtained. Again, broad distributions of the flavonoids in the membrane are obtained indicating the high dynamics of these molecules in the liquid-crystalline membrane.

Flavone appears to be almost entirely confined to the hydrocarbon chain region of the membrane (A). Within experimental error, no crosspeaks with the glycerol and headgroup region of the membrane are observed except for a small crosspeak with the γ protons of the headgroup indicating occasional upturns of the molecule. For chrysin, the distribution has its maximum in the upper chain region of the membrane (B). Both luteolin and myricetin show broad distributions in the membrane, which are biased towards the aqueous phase (C, D). The different magnitudes of the cross-relaxation rates indicate small differences in the correlation times of motion that modulates the cross-relaxation process.

The NOESY analysis also allows to determine the orientation of the flavonoids in the membrane by comparing the distribution profiles for different protons of the same flavonoid molecule. This is shown for luteolin (as the biologically most relevant molecule) in Fig. 6. The profiles

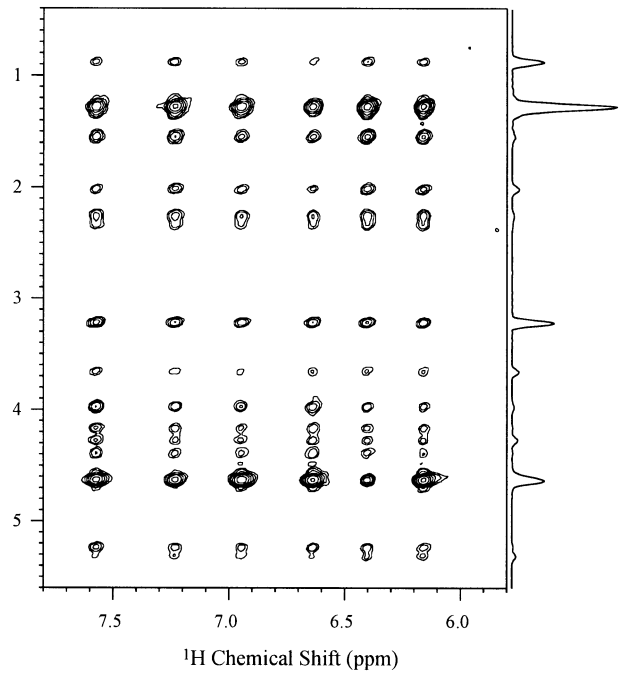

Fig. 4. Contour plot of the aromatic region of a ^{1}H MAS NOESY spectrum of a POPC/luteolin mixture at a mixing time of 300 ms and a water content of 40 wt.%. All crosspeaks have positive intensity.

demonstrate that the luteolin ring B (H 2′ /6′) is pointing towards the aqueous phase while ring A (H 6) is inserted deeper in the acyl chain region of the membrane. For myricetin, the same orientation can be determined (data not shown). In contrast, for chrysin an opposite orientation has been determined orienting the A ring with the two polar hydroxyl groups towards the aqueous phase. For flavone, the cross-relaxation data show no preferential orientation of the hydrophobic molecule in the membrane, indicating a high molecular mobility of flavone in the membrane.

3.2. Morphology of flavonoid/POPC membranes

To confirm that high concentrations of flavonoids do not alter the lamellar liquid-crystalline phase state of the bilayers, ^{31}P and ^{2}H NMR measurements have been carried out on selected samples (data not shown). Axially symmetric ^{31}P spectra have been obtained with a chemical shift anisotropy of $\Delta\sigma = 45.8$ ppm for pure POPC, $\Delta\sigma = 45.0$ ppm for POPC/flavone, and $\Delta\sigma = 42.2$ ppm for POPC/luteolin indicative of a lamellar liquid-crystalline phase state of the membranes. This is in agreement with the interface/headgroup localization of luteolin in membranes. Flavone on the other hand is localized more deeply in the membrane and, consequently, does not influence the lipid headgroups significantly.

^{2}H NMR results of perdeuterated POPC-d_{31} in the presence and absence of flavonoids indicated slightly increased order parameters in the upper chain in the presence of flavonoids (data not shown). Therefore, the high flavonoid concentrations used in this study do not influence the membrane morphology and phase state.

3.3. Lateral diffusion of flavonoids in membranes by PFG NMR

In order to study the mobility and lateral diffusion of the membrane bound flavonoid molecules, PFG NMR experi-

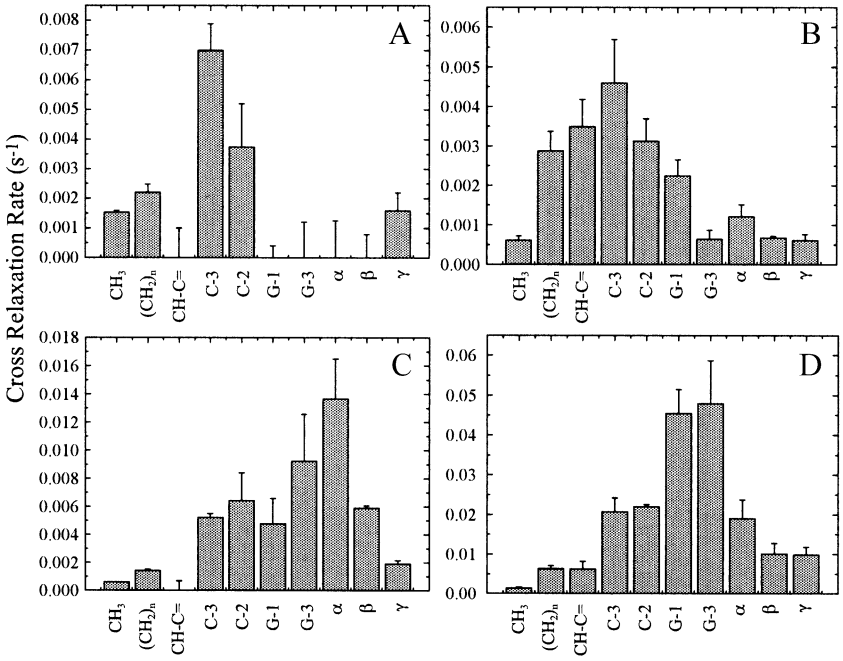

Fig. 5. Cross relaxation rates (s^{-1}) between the H 2′ /6′ protons of the B ring of flavonoid molecules with protons from POPC lipid segments in membranes at a POPC/flavonoid mixing ratio of 3:1. (A) flavone, (B) chrysin, (C) luteolin, and (D) myricetin.

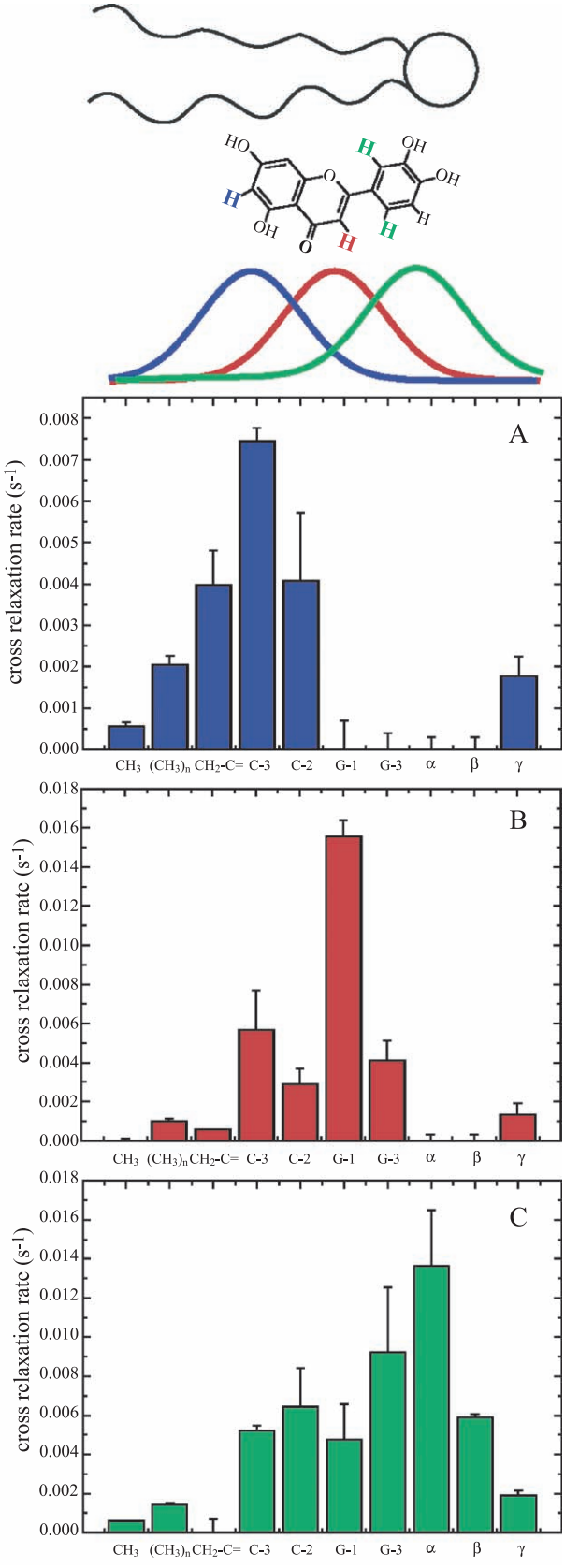

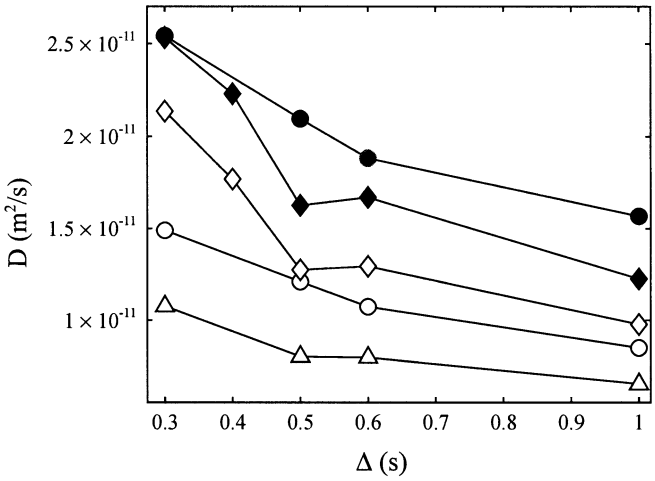

Fig. 7. Lateral diffusion coefficients of lipids (terminal CH_3 group, open symbols) and flavonoids (filled symbols) in POPC membranes as a function of the observation time at a temperature of 30 °C. The molar POPC/flavonoid mixing ratio was 10:1. Diamonds: flavone, circles: luteolin, triangles: myricetin.

ments have been performed at different observation times Δ. The spin echo amplitude of flavone, luteolin, and POPC protons follows an exponential decay as a function of the square of the gradient strength. Considering the low gradient strengths and the small diffusion coefficients, such a behavior is in agreement with two-dimensional diffusion of these molecules.

The data obtained for myricetin could not be described by a single exponent indicative of a two-dimensional diffusion process. The same behavior has also been observed for water. One can assume that for fast diffusing water molecules, the simple two-dimensional model is no longer valid because it does not consider contributions from spins diffusing along surfaces with very strong curvature or inside water pockets and bilayer defects. Such a behavior would also be relevant for myricetin, which apparently is weakly bound by the membrane and able to perform a faster diffusion of higher dimensionality similar to the weakly bound water molecules on the lipid surface.

Fig. 7 shows the diffusion coefficients of lipid and flavonoid molecules as a function of observation time as determined from the numerical analysis of the molecular diffusion. It should be noted that the real lateral diffusion coefficient D_L is somewhat larger then the coefficients obtained by fitting Eq. (2) at the rather long observations times used in our measurements. At longer observation times, membrane curvature and changes in the bilayer

Fig. 6. The cross relaxation rates (s^{-1}) between different luteolin protons and lipid segments of POPC in the presence of 25 mol% luteolin. The cross-relaxation rates provide the distribution functions of the (A) 6 position (ring A), (B) 3 position (ring C), and 2′ /6′ position (ring B) on the luteolin molecule. Above, a sketch of the approximate membrane location of luteolin is shown.

orientation result in a decrease of the observed diffusion coefficient [37]. Also NOE effects can result in the observation of a decreasing diffusion coefficient of the flavonoids [48]. The true lateral diffusion coefficient can be measured only for very short observation times. However, already this data characterizes the lateral diffusion of the POPC and the flavonoid molecules.

The diffusion coefficients observed for flavone and luteolin (filled symbols) are of the same magnitude as the diffusion coefficients of the POPC molecules (open symbols). This indicates that these flavonoids are rather well incorporated into the lipid membrane and move laterally on the same time scale as the lipid molecules. As the molecular weight of these molecules is lower, they diffuse slightly faster than the lipids. In contrast, myricetin shows a significantly faster diffusion that cannot be described by a two-dimensional model characteristic for membrane embedded molecules. Rather, the diffusion of myricetin is more comparable to that of membrane associated water molecules.

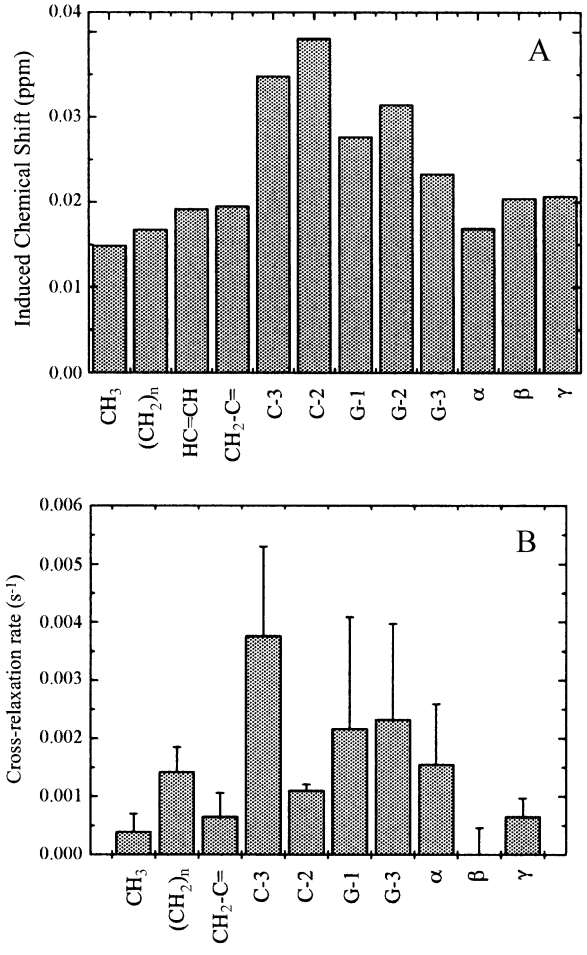

Fig. 8. (A) Induced ^{1}H chemical shifts (ppm) and cross-relaxation rates (s^{-1}) for luteolin-7-glucoside in POPC membranes at a concentration of 25 mol%. (B) Cross-relaxation rates (s^{-1}) between the 2′ /6′ protons on the B ring of luteolin-7-glucoside with POPC segments.

3.4. The interaction of luteolin-7-glucoside with lipid membranes

Finally, the membrane location of luteolin-7-glucoside has been determined. Due to the glycosylation, the flavonoid becomes more polar, which should modify its membrane binding properties. Induced chemical shift values and cross-relaxation rates with POPC molecules for luteolin-7-glucoside are shown in Fig. 8. The shape of the induced chemical shift and cross-relaxation profiles along the bilayer normal suggests a broader distribution for this molecule in the membrane compared to the other flavonoids of this study. However, we note that relatively small values are observed for both quantities, increasing the influence of experimental errors. From the NOESY data, it can be concluded that the carbon ring B is deeper inserted in the membrane compared to luteolin. The A ring with the attached glucoside ring is also oriented towards the aqueous environment. This is supported by the fact that the only intermolecular crosspeaks of the glucoside ring is observed with H_2O indicating the high affinity of the glucoside to the interbilayer water.

4. Discussion

4.1. Localization and distribution of flavonoids in lipid membranes

The aim of the current study was the detailed measurement of the localization of several flavonoid molecules with varying numbers of hydroxyl groups in lipid membranes. The hydrophobicity of the flavonoids decreases with an increasing number of OH groups [11]. All investigated flavonoids showed a propensity for the lipid membrane indicated by strong interactions with lipid segments. The NMR techniques applied in this study allowed to quantitatively determine the interaction strength between flavonoid and phospholipid segments. All flavonoids showed a broad distribution in the membrane, which was biased towards the hydrophobic core of the bilayer for the unpolar flavone and chrysin and towards the aqueous phase for the more polar luteolin and myricetin.

Such broad distributions are typically found for small membrane bound molecules [16–20] in agreement with modern membrane models characterized by a high degree of molecular disorder and structural heterogeneity [27,28]. However, defined maxima of the distributions indicate the average localization of the respective molecule. As the flavonoids became more hydrophilic, their membrane localization is more shifted towards the aqueous environment. This is in agreement with measurements of water/olive oil partitioning [11]. While flavone partitioned to 100% into the oil phase, only 96% and 34% oil partitioning was observed for chrysin und luteolin, respectively. These results correlate well with the increase of hydroxyl groups.

The average orientation of a respective flavonoid molecule in the membrane is mostly governed by its physical properties. For the rather unpolar flavone, which is mostly confined to the hydrocarbon region of the lipid membrane, no preferential orientation could be derived from the NOESY data. Therefore, a rapid reorientation of the molecule in the membrane is likely. For chrysin, luteolin, and myricetin, a maximum of the distribution in the lipid/water interface has been detected. The lipid/water interface is a broad region of the membrane including the headgroup, glycerol, and upper chain region. Because of its complex electrostatic and hydrogen bonded structure, the membrane interface provides the perfect environment to host small partially polar molecules [17,49]. Thus, the hydroxyl groups of the flavonoid molecules are involved in the hydrogen bond networks of the lipid/water interface [12]. In particular, hydrogen bonds with the C═O groups and the phosphate group of the phospholipid molecules are formed. Further favorable interactions between flavonoid and lipid molecules involve charge-dipole and dipole–dipole interactions [50] as flavonoids have a relatively strong dipole moment between 3.6 and 6.6 D for the investigated molecules. Finally, cation–π interactions may contribute to the lowest free energy location of chrysin, luteolin, and myricetin in the lipid/water interface of the bilayer [17,51]. This interface location of flavonoids may be responsible for the membrane destabilization upon flavonoid binding that has been discussed in literature [11–13].

In spite of the various flavonoid phospholipid interactions, the amplitude of transverse motions of the flavonoids is rather big, indicating that there is no explicit binding site for flavonoids but rather a dynamic penetration of lower membrane regions. This is confirmed by the PFG NMR investigations that revealed the lateral diffusion properties of the flavonoids. The most polar myricetin appears to be both membrane-associated and water-solved as it showed the typical signatures of the diffusion of water molecules in the proximity of a lipid surface [37]. The other flavonoids are more confined to the membrane environment and exhibit similar lateral diffusion behavior as the phospholipid molecules. Due to their lower molecular weight, slightly larger diffusion coefficients have been observed.

In plants, most of the flavonoids are present in the glycosylated form [11]. Therefore, we have also investigated membrane partitioning and orientation of luteolin-7-glucoside. Due to the sugar modification of the 7 position of the A ring of luteolin (see Fig. 1), the molecule acquires a very hydrophilic center that is facing the aqueous environment. Accordingly, a much broader distribution of the hydrophobic anchor of the molecule in the membrane is obtained as a result of the more pronounced dynamics of the molecule. These motions allow for intense contacts of luteolin-7-glucoside with all segments of the POPC molecules in the lipid membrane. Indeed, the antioxidative capacity of luteolin-7-glucoside against lipid peroxidation remains comparable to that of luteolin [52], while the glucoside is less active than the aglycon in reducing cholesterol biosynthesis [53], which presumably is exerted via interaction with protein kinases [5].

To obtain the data presented in this paper, rather high flavonoid concentrations had to be applied for technical reasons. To confirm the lamellar liquid-crystalline phase state of the bilayers in the presence of such high flavonoid concentrations, we have carried out static ^{31}P and ^{2}H NMR measurements. No significant alterations of the bilayer structure have been found, indicating that liquid-crystalline bilayers can easily accommodate high concentrations of flavonoid molecules. Only very moderate changes in headgroup orientation and chain packing result from flavonoid binding.

An additional concern is the aggregation of flavonoid molecules at high concentration. However, the very narrow line width of the flavonoid signals in the ^{1}H MAS NMR spectra suggests that no aggregation has taken place in our samples. Further, membrane-associated flavonoids diffuse faster than lipid molecules, which is in agreement with the smaller molecular weight of these monomeric compounds. Therefore, we can conclude that high concentrations of flavonoids do not induce aggregation of these compounds.

4.2. Biological implications

The antioxidant activity of flavonoid molecules appears to depend on their structure and ability to interact with and penetrate the lipid membrane [15]. In this paper, we have determined the average location of flavonoid molecules with varying degrees of hydroxylation in lipid bilayers. Generally, a broad distribution of these molecules along the long axis of the phospholipids has been found. It has already been suggested that the antioxidant properties of flavonoids are modulated by the location of these molecules in the membrane [10]. The number and position of the flavonoid hydroxyl groups not only donate hydrogen atoms to scavenge free radicals but also determine the membrane localization and distribution of the molecules. Due to their broad dynamic distribution in the membrane, flavonoids can access all segments of the lipid molecules, thus efficiently preventing peroxidation. It is interesting that in the glycosylated form (in position 7), flavonoids are still distributed over the entire membrane to protect any given double bonds from oxidation. The same may be true for glucuronidated flavonoids that may occur during biotransformation [54], thus maintaining the antioxidative potential. In combination with the metal ion chelating properties of the π electron system of the aromatic ring, nature has come up with very potent inhibitors of lipid peroxidation that are promising molecules for further pharmaceutical developments.

Acknowledgements

The junior research group is funded by the Saxon State Ministry of Higher Education, Research and Culture.

References

[1] C.A. Rice-Evans, N.J. Miller, G. Paganga, Structure–antioxidant activity relationships of flavonoids and phenolic acids, Free Radic. Biol. Med. 20 (1996) 933–956.
[2] S.A. van Acker, D.J. van den Berg, M.N. Tromp, D.H. Griffioen, W.P. van Bennekom, W.J. van der Vijgh, A. Bast, Structural aspects of antioxidant activity of flavonoids, Free Radic. Biol. Med. 20 (1996) 331–342.
[3] R. Kahl, Protective and adverse biological actions of phenolic antioxidants, in: H. Sies (Ed.), Oxidative Stress: Oxidants and Antioxidants, Academic Press, London, 1991, pp. 245–273.
[4] E. Middleton Jr., C. Kandaswami, The impact of plant flavonoids on mammalian biology: implications for immunity, inflammation and cancer, in: J.B. Harbone (Ed.), The Flavonoids: Advances in Research Since 1986, Chapman & Hall, London, 1993, pp. 619–652.
[5] R. Gebhardt, Prevention of taurolithocholate-induced hepatic bile canalicular distortions by HPLC-characterized extracts of artichoke (*Cynara scolymus*) leaves, Planta Med. 68 (2002) 776–779.
[6] F.V. So, N. Guthrie, A.F. Chambers, M. Moussa, K.K. Carroll, Inhibition of human breast cancer cell proliferation and delay of mammary tumorigenesis by flavonoids and citrus juices, Nutr. Cancer 26 (1996) 167–181.
[7] P.G. Pietta, Flavonoids as antioxidants, J. Nat. Prod. 63 (2000) 1035–1042.
[8] A.B. Hendrich, R. Malon, A. Pola, Y. Shirataki, N. Motohashi, K. Michalak, Differential interaction of *Sophora* isoflavonoids with lipid bilayers, Eur. J. Pharm. Sci. 16 (2002) 201–208.
[9] K. Wojtowicz, B. Pawlikowska-Pawlega, A. Gawron, L.E. Misiak, W.I. Gruszecki, Modifying effect of quercetin on the lipid membrane, Folia Histochem, Cytobiolologie 34 (Suppl. 1) (1996) 49–50.
[10] A. Arora, T.M. Byrem, M.G. Nair, G.M. Strasburg, Modulation of liposomal membrane fluidity by flavonoids and isoflavonoids, Arch. Biochem. Biophys. 373 (2000) 102–109.
[11] C. van Dijk, A.J. Driessen, K. Recourt, The uncoupling efficiency and affinity of flavonoids for vesicles, Biochem. Pharmacol. 60 (2000) 1593–1600.
[12] F. Ollila, K. Halling, P. Vuorela, H. Vuorela, J.P. Slotte, Characterization of flavonoid–biomembrane interactions, Arch. Biochem. Biophys. 399 (2002) 103–108.
[13] L. Movileanu, I. Neagoe, M.L. Flonta, Interaction of the antioxidant flavonoid quercetin with planar lipid bilayers, Int. J. Pharm. 205 (2000) 135–146.
[14] B. Yang, A. Kotani, K. Arai, F. Kusu, Estimation of the antioxidant activities of flavonoids from their oxidation potentials, Anal. Sci. 17 (2001) 599–604.
[15] A.C. Santos, S.A. Uyemura, J.L. Lopes, J.N. Bazon, F.E. Mingatto, C. Curti, Effect of naturally occurring flavonoids on lipid peroxidation and membrane permeability transition in mitochondria, Free Radic. Biol. Med. 24 (1998) 1455–1461.
[16] L.L. Holte, K. Gawrisch, Determining ethanol distribution in phospholipid multilayers with MAS-NOESY spectra, Biochemistry 36 (1997) 4669–4674.
[17] W.M. Yau, W.C. Wimley, K. Gawrisch, S.H. White, The preference of tryptophan for membrane interfaces, Biochemistry 37 (1998) 14713–14718.
[18] S.E. Feller, C.A. Brown, D.T. Nizza, K. Gawrisch, Nuclear overhauser enhancement spectroscopy cross-relaxation rates and ethanol distribution across membranes, Biophys. J. 82 (2002) 1396–1404.
[19] D. Huster, P. Müller, K. Arnold, A. Herrmann, Dynamics of membrane penetration of the fluorescent 7-nitrobenz-2-oxa-1,3-diazol-4-yl (NBD) group attached to an acyl chain of phosphatidylcholine, Biophys. J. 80 (2001) 822–831.
[20] D. Huster, P. Müller, K. Arnold, A. Herrmann, The distribution of chain attached NBD in acidic membranes determined by ^{1}H MAS NMR spectroscopy, Eur. Biophys. J. 32 (2003) 47–54.
[21] J. Forbes, C. Husted, E. Oldfield, High-field, high-resolution proton "magic-angle" sample-spinning nuclear magnetic resonance spectroscopic studies of gel and liquid crystalline lipid bilayers and the effects of cholesterol, J. Am. Chem. Soc. 110 (1988) 1059–1065.
[22] K. Wüthrich, NMR of Proteins and Nucleic Acids, Wiley, New York, 1986.
[23] J. Forbes, J. Bowers, X. Shan, L. Moran, E. Oldfield, M.A. Moscarello, Some new developments in solid-state nuclear magnetic resonance spectroscopic studies of lipids and biological membranes, including the effect of cholesterol in model and natural systems, J. Chem. Soc., Faraday Trans. 1 (84) (1988) 3821–3849.
[24] Z.J. Chen, R.E. Stark, Evaluating spin diffusion in MAS-NOESY spectra of phospholipid multibilayers, Solid State Nucl. Magn. Reson. 7 (1996) 239–246.
[25] D. Huster, K. Arnold, K. Gawrisch, Investigation of lipid organization in biological membranes by two-dimensional nuclear Overhauser enhancement spectroscopy, J. Phys. Chem., B 103 (1999) 243–251.
[26] D. Huster, K. Gawrisch, NOESY NMR crosspeaks between lipid headgroups and hydrocarbon chains: spin diffusion or molecular disorder? J. Am. Chem. Soc. 121 (1999) 1992–1993.
[27] M.C. Wiener, S.H. White, Structure of a fluid dioleoylphosphatidylcholine bilayer determined by joint refinement of X-ray and neutron diffraction data III. Complete structure, Biophys. J. 61 (1992) 434–447.
[28] S.H. White, M.C. Wiener, The liquid-crystallographic structure of fluid lipid bilayer membranes, in: K.M. Merz, B. Roux (Eds.), Biological Membranes. A Molecular Perspective from Computation and Experiment, Birkhäuser, Boston, 1996, pp. 127–144.
[29] S.E. Feller, D. Huster, K. Gawrisch, Interpretation of NOESY cross-relaxation rates from molecular dynamics simulations of a lipid bilayer, J. Am. Chem. Soc. 121 (1999) 8963–8964.
[30] R.M. Venable, Y. Zhang, B.J. Hardy, R.W. Pastor, Molecular dynamics simulations of a lipid bilayer and of hexadecane: an investigation of membrane fluidity, Science 262 (1993) 223–226.
[31] D. Huster, K. Arnold, K. Gawrisch, Influence of docosahexaenoic acid and cholesterol on lateral lipid organization in phospholipid membranes, Biochemistry 37 (1998) 17299–17308.
[32] D. Huster, K. Kuhn, D. Kadereit, H. Waldmann, K. Arnold, High resolution magic angle spinning NMR for the investigation of a ras lipopeptide in a lipid bilayer, Angew. Chem., Int. Ed. 40 (2001) 1056–1058.
[33] D. Huster, A. Vogel, C. Katzka, H.A. Scheidt, H. Binder, S. Dante, T. Gutberlet, O. Zschörnig, H. Waldmann, K. Arnold, Membrane insertion of a lipidated ras peptide studied by FTIR, solid-state NMR, and neutron diffraction spectroscopy, J. Am. Chem. Soc. 125 (2003) 4070–4079.
[34] C. Le Guerneve, M. Seigneuret, High-resolution mono- and multidimensional magic angle spinning ^{1}H nuclear magnetic resonance of membrane peptides in nondeuterated lipid membranes and H_2O, Biophys. J. 71 (1996) 2633–2644.
[35] W. Zhang, E. Crocker, S. Mc Laughlin, S.O. Smith, Binding of peptides with basic and aromatic residues to bilayer membranes: phenylalanine in the MARCKS effector domain penetrates into the hydrophobic core of the bilayer, J. Biol. Chem. 278 (2003) 21459–21466.
[36] F. Volke, A. Pampel, Membrane hydration and structure on a subnanometer scale as seen by high resolution solid state nuclear magnetic resonance: POPC and POPC/$C_{12}EO_4$ model membranes, Biophys. J. 68 (1995) 1960–1965.
[37] A. Pampel, J. Kärger, D. Michel, Lateral diffusion of a transmem-

brane peptide in lipid bilayers studied by pulsed field gradient NMR in combination with magic angle sample spinning, Chem. Phys. Lett. 379 (2003) 555–561.
[38] H.C. Gaede, K. Gawrisch, Lateral diffusion rates of lipid, water, and a hydrophobic drug in a multilamellar liposome, Biophys. J. 85 (2003) 1734–1740.
[39] I. Wawer, A. Zielinska, ^{13}C CP/MAS NMR studies of flavonoids, Magn. Reson. Chem. 39 (2001) 374–380.
[40] C.A. Kingsbury, J.H. Looker, C-13 spectra of methoxyflavones, J. Org. Chem. 40 (1975) 1120–1124.
[41] J.H. Davis, K.R. Jeffrey, M. Bloom, M.I. Valic, T.P. Higgs, Quadrupolar echo deuteron magnetic resonance spectroscopy in ordered hydrocarbon chains, Chem. Phys. Lett. 42 (1976) 390–394.
[42] M.A. Mc Cabe, S.R. Wassall, Fast-Fourier-transform DePaking, J. Magn. Reson., B 106 (1995) 80–82.
[43] M. Lafleur, B. Fine, E. Sternin, P.R. Cullis, M. Bloom, Smoothed orientational order profile of lipid bilayers by ^{2}H-nuclear magnetic resonance, Biophys. J. 56 (1989) 1037–1041.
[44] J. Jeener, B.H. Meier, P. Bachmann, R.R. Ernst, Investigation of exchange processes by two-dimensional NMR spectroscopy, J. Chem. Phys. 71 (1979) 4546–4553.
[45] S. Macura, R.R. Ernst, Elucidation of cross relaxation in liquids by two-dimensional N.M.R. spectroscopy, Mol. Phys. 41 (1980) 95–117.
[46] D. Wu, A. Chen, C.S. Johnson Jr., An improved diffusion-ordered spectroscopy experiment incorporating bipolar-gradient pulses, J. Magn. Reson., A 115 (1995) 260–264.
[47] H. Stamm, H. Jäckel, Relative ring-current effects based on a new model for aromatic-solvent-induced shifts, J. Am. Chem. Soc. 111 (1989) 6544–6550.
[48] A. Chen, M. Shapiro, Nuclear overhauser effects on diffusion measurements, J. Am. Chem. Soc. 121 (1999) 5338–5339.
[49] W.C. Wimley, S.H. White, Experimentally determined hydrophobicity scale for proteins at membrane interfaces, Nat. Struct. Biol. 3 (1996) 842–848.
[50] J.N. Israelachvili, Intermolecular and Surface Forces, Academic Press, London, 1992.
[51] D.A. Dougherty, Cation–pi interactions in chemistry and biology: a new view of benzene, Phe, Tyr, and Trp, Science 271 (1996) 163–168.
[52] R. Gebhardt, M. Fausel, Antioxidant and hepatoprotective effects of artichoke extracts and constituents in cultured rat hepatocytes, Toxicol. In Vitro 11 (1997) 669–672.
[53] R. Gebhardt, Inhibition of cholesterol biosynthesis in primary cultured rat hepatocytes by artichoke (*Cynara scolymus* L.) extracts, J. Pharmacol. Exp. Ther. 286 (1998) 1122–1128.
[54] C. Manach, C. Morand, V. Crespy, C. Demigne, O. Texier, F. Regerat, C. Remesy, Quercetin is recovered in human plasma as conjugated derivatives which retain antioxidant properties, FEBS Lett. 426 (1998) 331–336.